AN EXPERIMENTAL AND THEORETICAL STUDY OF WEB TRACTION OVER A NONVENTED ROLLER

by

B. S. Rice[1], K. A. Cole[1] and S. Müftü[2]
[1]Eastman Kodak Company
[2]M.I.T. Haystack Observatory
USA

ABSTRACT

The traction developed between a thin flexible web, wrapped around a nonvented, rotating cylindrical roller is studied experimentally and theoretically. A series of eight webs representing a wide range of surface roughness characteristics are traction tested against the same roller over a wide speed range. A one-dimensional finite difference model that couples air film pressure (Reynold's equation), web bending and solid-body contact using an asperity compliance function is used to model the experimental traction data. An optimization technique is used to estimate the asperity compliance function parameters. A new model for computing the asperity engagement height for non-Gaussian surfaces is presented when the roughness of both surfaces is taken into account. Results are presented which indicate the viability and utility of the new methods.

NOMENCLATURE

A	contact area
b	characteristic bending length
c	web thickness
D	bending stiffness of the web
ε	error function
E	Young's modulus of elasticity
h	web-to-roller clearance
H	Heaviside step function
k	shell stiffness of the web
L	length of the web
p	air pressure under the web
P_{atm}	atmospheric pressure

P_c web-to-roller contact pressure
R roller radius
R_{pm} surface roughness parameter, average of the five highest peaks in the sample, measured from the mean plane
R_z surface roughness parameter, difference between the average of the five highest peaks and the five lowest valleys in the sample, measured from the mean plane
T web tension per unit width
V transport velocity
w web displacement
w_q quiescent web displacement
α asperity engagement height parameter
β asperity compliance parameter
δ function used in defining web roller spacing
ΔT roller tension difference on the dynamic traction tester
θ roller wrap angle
λ_a molecular mean-free path of air
μ kinetic coefficient of friction
μ_a air viscosity
ν Poisson's ratio
ρ mass density of the web

Subscripts

a average tension
c combined web and roller
d dynamic traction tester
i, e roller entrance, exit
m model
o low speed, 0.005 m/s
r roller
w web

INTRODUCTION

A model is presented in this paper for computing the traction behavior of a web conveyed over a cylindrical, rotating roller (Figure 1). The successful use of rollers is contingent on maintaining intimate contact between the roller and web during transport. One physical effect which can act to degrade performance is air entrainment (Daly, 1965). During web transport, air is carried along the web and the roller due to the "no-slip" condition at the web and roller surfaces. The converging geometry of the web/roller interface then acts as a wedge leading to the development of increased air pressure between the web and roller. This causes the web to partially lift away from the roller leading to a loss in traction between the web and the roller. Relative motion due to traction loss may lead to physical defects on the web such as scratches.

The traction performance of cylindrical rollers are strongly influenced by web and roller roughness, with the smoother web/roller systems losing traction as a function of speed more rapidly than rougher systems. It is not uncommon to include additives onto the web to modify both the friction and roughness characteristics of the web to help

reduce traction loss sensitivity (Forrest and Anderson, 1997). At higher speeds, such a simple design is no longer adequate and design modifications must be provided to mitigate the effect of air entrainment. One example is to provide grooves in the cylindrical roller to provide air pressure relief: the active venting method provides better performance over a higher speed range and helps to reduce traction sensitivity to roller and web roughness.

An accurate model for web to nonvented roller traction is a necessary first step in the development of a vented roller traction model since in standard grooved designs, the web and land area roughness can still influence the traction performance. Furthermore many applications still rely on nonvented rollers and in such cases, a model will provide the capability to estimate traction performance for proposed webs and rollers before they are manufactured.

Traction can be presented in two general ways. The first method is to state traction as the amount of tension difference that the roller can sustain before gross slip is incurred between the web and roller. At very low speeds, the tension difference is a maximum and is related to the low speed kinetic coefficient of friction, μ_o, by the well known belt-wrap formula which relates the belt-wrap pressure, *T/R*, to the tension increase,

$$\mu_o = \frac{1}{\theta} ln\left(\frac{T_{eo}}{T_{io}}\right), \qquad \{1\}$$

where θ is the wrap angle, T_{io} is the entrance tension and T_{eo} is the exit tension. The tension difference, ΔT_{ao}, is the difference between the entrance and exit tensions.

The tension difference at increased speeds, T_e - T_i, decreases owing to partial air film support. This leads to an alternative presentation of the traction data in terms of an *equivalent high speed kinetic coefficient of friction*, μ_d, where the measured tension change is used in the belt-wrap formula,

$$\mu_d = \frac{1}{\theta} ln\left(\frac{T_e}{Ti}\right), \qquad \{2\}$$

and the partial air support causes μ_d to decease relative to μ_o. Traction data has been presented both ways in the literature. Knox and Sweeney (1971) present experimental data in terms of tension differences while Ducotey and Good (1995) show data in terms of an equivalent friction coefficient. Both of these studies provide typical examples where the influence of such web handling parameters such as speed, web tension and roller radius were investigated.

Knox and Sweeney (1971) also sought to provide a model to relate roller traction to offline web-to-roller pressure/clearance zero speed measurements. The air film thickness was modeled using the foil bearing equation (Eshel and Elrod, 1965) which is derived by treating the web as an infinitely wide membrane and the air film using a simplified Reynold's equation where air compressibility is neglected. Web-to-roller contact, which

typically occurs at asperities on the surfaces, was not modeled. Instead, comparisons were made between predicted clearances assuming no contact and the off-line measurements. Good correlation was seen between the two measurements. This led to the observation that a few large asperities are more important for achieving high roller traction than a large number of small asperities. No attempt was made to relate the findings to roughness measurements or to consider both surfaces to be rough.

Müftü and Altan (1999) have provided a model which considers the effects of asperity contact on the traction loss of a porous web moving over a cylindrical stationary guide. The air film is modeled using a simplified Reynold's equation accounting for web porosity and compressible air flow (Müftü and Benson, 1995). The web is modeled using a formulation which accounts for moderately large web deformations and provides a self-adjusting reference state (Müftü and Cole, 1998). By this means, web strains are measured from the quiescent contact equilibrium state of the web, rather than from an ideally smooth reference surface. Contact between the two surfaces is treated using an empirically based asperity compliance function. This function has been used for the head-tape interface problem (Wu and Talke, 1996) and is also referred to as the parabolic contact model,

$$P_c = \beta\left(1-\frac{h}{\alpha}\right)^2\left[1-H(h-\alpha)\right], \qquad \{3\}$$

where β is the asperity compliance parameter and α is the asperity engagement height. The function H insures that contact pressure, P_C, is not applied if the web-to-roller clearance, h, is greater than α. Müftü and Altan (1999) present the traction results in terms of tension differences. Effects of permeability, asperity compliance and engagement height are studied. But, no attempt is made to relate the contact parameters to off-line roughness measurements.

The parabolic contact model presented by Wu and Talke assumes that only one surface is rough. Greenwood and Tripp (1971) present a model which considers both surfaces to be rough. This model assumes that the distribution of the surface asperity heights are Gaussian and so has the benefit of being non-empirical. However, measuring parameters for the model is difficult and further, the Gaussian assumption limits the applicability of the model.

It has been shown that magnetic tapes and recording heads typically can be put into one of these two categories; i.e. parabolic or GT model (Wu and Talke, 1996; Bhushan, 1996). However, in roller conveyance the range of web and roller surface roughness is almost infinite. This leads to an obvious need for not only an appropriate contact model when both surfaces are rough but also to a need for a method to determine the parameters of such a model. The parabolic model does not have the Gaussian restriction of the Greenwood and Tripp model, therefore it has been selected for this work.

The purpose of this paper is to provide a simple experimental methodology to estimate the asperity compliance and the asperity engagement height parameters for the parabolic contact model when the roughness of one or both surfaces is taken into

account. A series of eight webs representing a wide range of surface roughness characteristics are traction tested against a rotating cylindrical roller over a wide speed range. Müftü and Altan's model (1999) is used to simulate the experimental traction data. The model is then used to generate optimum estimates of the contact model parameters.

Web and roller surface roughness parameters are measured using an optical surface analyzer and web asperity compliance is measured using a stack compression test. These measured parameters are then used to develop coefficients for the parabolic contact model and are compared to the optimized coefficients predicted by the model.

ANALYTICAL TRACTION MODEL

Air Pressure/Web Displacement Equations

The equations used to simulate the measured roller traction results are presented in this section. Air lubrication due to the motion of the roller and the web is modeled using the first-order modified Reynold's equation. For an infinitely wide compressible bearing this equation becomes,

$$\frac{\partial}{\partial x}\left[ph^3\frac{\partial p}{\partial x}\left(1+6\frac{\lambda_a}{h}\right)\right]=6\mu_a\left(V_w+V_r\right)\frac{\partial ph}{\partial x}, \qquad \{4\}$$

where p is the air pressure in the clearance, λ_a is the molecular mean-free path of air, μ_a is the air viscosity and V_W and V_r are the web and roller velocities (Burgdorfer, 1959). The edges of the lubrication zone are located at points B and E as shown in Figure 1. At these locations, the air pressure is set equal to the ambient air pressure, P_{atm}.

When an initially flat web is wrapped around a roller with radius R, under tension T, its radius of curvature along a coordinate axis placed on the web is given by (Müftü and Cole, 1998),

$$\frac{1}{R(x)}=\frac{1}{R}\begin{cases} e^{-\left(1+\left(x_C-x\right)/b\right)}, & 0\le x\le x_C \\ 1, & x_C\le x\le x_D \\ e^{-\left(1+\left(x-x_D\right)/b\right)}, & x_D\le x\le L \end{cases} \qquad \{5\}$$

where $b=(D/T)^{1/2}$ is the characteristic bending length and $D=Ec^3/12(1-\nu^2)$ is the bending stiffness, calculated by using the elastic modulus E, Poisson's ratio ν and thickness c of the web. The web wraps the roller between the tangency points C and D and has a wrap length of $R\theta$. The web curvature causes the curved part of the web to gain an additional in-plane shell stiffness, $k=Ec/R(x)^2(1-\nu^2)$ and belt-wrap pressure, $T/R(x)$ acting radially inward.

These two effects along with membrane and bending stiffness are balanced by external air and contact pressure. These effects can be combined to yield the following

differential equation for the normal displacement of the web, w, with respect to the roller (Müftü and Altan, 1999),

$$D\frac{d^4\left(w-w_q\right)}{dx^4}+k\left(w-w_q\right)+\left(\rho V_w^2-T\right)\frac{d^2\left(w-w_q\right)}{dx^2}=\left(p-P_{atm}\right)+P_c-\frac{T}{R(x)}, \quad \{6\}$$

where ρ is the mass density per unit area of the web and w_q is the quiescent ($V_w, V_r=0$) web displacement. By formulating the differential equation in this way, inaccuracies are avoided which would otherwise arise when rough surfaces ($\alpha \approx 5$ μm or higher), which are common in web-roller traction applications, are considered. Physically, this is equivalent to allowing the web to settle on the asperity peaks without an attendant tension increase. Simple support conditions are assumed at the boundaries. The web-roller clearance is given by,

$$h = w+\delta, \quad \{7\}$$

where δ is a function representing the shape of the roller in the x coordinate (Müftü and Altan, 1999).

Equations {3}, {4}, {6}, and {7} along with the appropriate boundary conditions describe the mechanics of a web conveying over a rotating cylindrical roller. A stacked iteration scheme where each equation is solved sequentially is employed to solve these equations. Equations {4} and {6} are discretized using standard finite-difference techniques and solved, since the system is nonlinear, by Newton's method (Müftü and Benson, 1995). The solution algorithm is composed of two sweeps. In the first one, the air pressure calculations are turned off and the quiescent solution determined. The web displacement w_q determined in this step is then substituted into equation {6} and the coupled equations solved to yield the complete solution.

Typical output from the coupled model is shown in Figure 2. Here, air film height, h, in the wrap zone is shown plotted against roller circumferential position. Results are presented for three speeds: 0.70, 0.75, and 0.80 m/s. The roller radius is 0.0508 m, the roller wrap angle is 90°, the web thickness is 10 μm, mass density is zero and the tension is 175 N/m. The asperity engagement height parameter is 3 μm and the asperity compliance parameter is 10 MPa. The grid spacing used in this example and in later simulations is 50 μm.

The predicted results show that as speed is increased, the web deflection increases as expected. The web is fully in contact with the roller at 0.7 and 0.75 m/s where the asperities are compressed to 2.98 μm. It is further seen that the web begins to be fully air supported at a speed between 0.75 and 0.80 m/s where the web clears the asperity engagement height. This agrees very favorably with the predictions using the foil bearing equation, $h=.643R(6\mu_a(V_W+V_r)/T)^{2/3}$, (Eshel and Elrod, 1965) which yields a web speed of 0.74 m/s for a clearance of 3 μm. The results also indicate that the trailing edge flies at a lower clearance relative to the entry and midwrap regions due to the negative air pressure (not shown) that characteristically develops at the exit side of a foil

bearing (Gross, 1980). This behavior will have the effect of delaying complete web-to-roller traction loss to higher speeds than would be predicted using the simple foil bearing.

Computation of the Equivalent Coefficient of Friction

In this work, a macroscopic approach is taken to evaluate the equivalent coefficient of friction using the model. This approach makes the assumption that the equivalent coefficient of friction is linearly related to the contact force, F_C, which is found by integrating the contact pressure over the contact area, A, and inversely related to the belt wrap force, F_b, which is also found by integration of the belt wrap pressure,

$$F_C = \int_A P_C dA, \; F_b = \int_A {}^{T}\!/_{R} \, dA . \qquad \{8\}$$

In this fashion, the equivalent coefficient of friction as predicted by the model μ_m can be written in terms of the low speed kinetic coefficient of friction as,

$$\mu_m = \mu_o \frac{F_c}{F_b} . \qquad \{9\}$$

Lastly, since the model does not consider the effect in changes of tension around the wrap, the midwrap tension is therefore used in equations {6} and {8},

$$T = T_a = \frac{T_e + T_i}{2} . \qquad \{10\}$$

EXPERIMENTAL MEASUREMENTS & RESULTS

A series of eight webs were traction tested experimentally: one polyethylene coated paper, one cellulose triacetate (CTA) and five polyethylene terephthalate (PET) films. The PET webs had a wide range of coatings which caused significant surface roughness differences between them. A description of each web is provided in Table 1. A nonvented anodized aluminum roller with a radius of 50.8 mm and length of 1.5 m was used in all the tests.

Several measurements were made to provide data to develop and validate the surface roughness contact model:

- narrow width slow speed kinetic coefficient of friction between the roller and webs,
- full width high speed equivalent coefficient of friction between the roller and webs,
- surface roughness of the webs and roller,
- stack compression measurements for three of the eight webs.

Low Speed Kinetic Coefficient of Friction - Narrow Width

The kinetic coefficient of friction of the web-to-roller system was measured for all eight webs using a standard ASTM (G143-96) test. For each web, three 25 mm wide strips were removed from different widthwise locations from the high speed full width

sample. Each strip was tested using the following conditions: 90° wrap, 87.5 N/m low side tension and a slip speed of 5 mm/s with the roller held stationary. The measurements were made at 70°F and 40% relative humidity. The average kinetic coefficient of friction for each web is shown in the first row of Table 2. The 95% confidence limits are ± 0.01. The average tension, T_a, during the measurements was 103 N/m.

High Speed Equivalent Coefficient of Friction - Full Width

The equivalent coefficient of friction between all 8 webs and the roller were measured at speeds ranging from 0.13 to 12.5 m/s. Figure 3 shows the device used to measure the full width high speed equivalent coefficient of friction. This device, referred to as the dynamic traction tester, operates in an endless band mode. All the webs were tested at standard conditions (70°F, 50%) and were 0.75 m wide and 30 m long. At each test point an increasing torque was applied to the test roller until a 0.03% speed difference between the web and the roller was achieved. This was repeated three times. The value of μ_d was computed from the average of the three torque values using equation {2}. Based on the location of the tension setting device (float roller) the exit tension was fixed at 175 N/m and the entrance tension drops in proportion to the applied torque to the roller. For a wrap angle of 90° and an equivalent coefficient of friction of 0.25 the average unit tension, T_a, is 147 N/m. Results for all eight webs are listed in Table 2. The 95% confidence limits are +/- 0.01.

The equivalent coefficient of friction values for webs 1 through 3 at 0.25 and 0.13 m/s are higher than the 0.005 m/s measurements based on the 95% confidence limits. Clearly the low speed measurements are not representative of the high speed measurements for these three webs. Some possible explanations for these differences are widthwise variations in low speed kinetic coefficient of friction, relative humidity differences between the two tests, and variations in average tension between the two tests.

The lowest speed at which the dynamic traction tester can be used reliably is 0.13 m/s. For several webs the lowest test speed was 0.25 m/s or greater. Since traction drops off so rapidly with increasing speed, it was not possible to use the lowest speed equivalent coefficient of friction measured from the dynamic traction test to estimate the friction at 0.005 m/s. For web 1 the values of friction at 0.005 and 0.25 m/s were so widely different that the 0.33 value was used for μ_o. For the other seven webs the equivalent coefficient of friction from the ASTM G143 tester were used for μ_o. The effects of errors in the low speed kinetic coefficient of friction will be discussed in detail in the numerical results section.

Web/Roller Surface Roughness

Web and roller surface roughness was measured using a commercially available optical surface profiler. Sample size was 460 μm by 600 μm with an 820 nm resolution. For each web, four locations across the width were measured. Values were reported at each location and were the average of five samples made within 10 mm of each other (20 samples measured on each web). Table 3 shows the overall average, standard deviation and 95% confidence limits for all eight webs. Two roughness measures are reported: the average of the highest peaks in the sample with respect to the mean plane, R_{pm} and; the

difference between the average of the five highest peaks and five lowest valleys in the sample measured from the mean plane, R_z. For the roller, two locations were measured: one near the roller center and the other 0.375 m from the center of the roller. The values reported at each location were again the average of five readings made within 10 mm of each other (10 readings made on the roller). The overall averaged results are shown in Table 3.

Stack Compression Measurements

Stack compression was measured for webs 1,5 and 8. This test consists of measuring the load/displacement behavior of a stack of individual plies 12.7 mm by 50.8 mm cut from each web. Three stacks of height 5.1 mm were tested for each web and the results averaged after being normalized to a per ply basis. This data was then used to estimate β. The computed values of β for webs 1,5 and 8 are 20850 Pa, 12500 Pa and 88800 Pa respectively. This assumes that both front and back surfaces have equal stiffness and the roller surface roughness has no influence on compliance. Both assumptions can lead to obvious errors, but as will be shown in the next section, β has only a secondary effect on traction. The estimates were obtained by regressing the experimental data using equation {3}. In the stack compression tests, displacements were measured relative to zero pressure and the asperity engagement parameter α_c was set to the measured values determined in the next section.

THE CONTACT PARAMETERS

The empirical parabolic contact pressure model given by equation {3} involves the asperity engagement height α and the asperity compliance β. In this section the following are discussed:

- a method for determining these two parameters, based on minimizing the equivalent coefficient of friction error between the experiments and the model,
- description of a new model to define the asperity engagement height α, based on easily measurable surface topography parameters,
- a heuristic formula for calculating the composite engagement height of two rough surfaces.

Determination of Contact Parameters Based on Traction Experiments and Model

If it is assumed that the surface asperities deform according to a parabolic model as given by equation {3}, then it would be possible to determine the α and β of this model from the experimentally measured coefficient of friction values, μ_d. This can be achieved by minimizing the squared-error ε^2 between the experimental, μ_d, and predicted, μ_m, coefficient of friction values, over the tested web speeds, by varying α and β. The squared-error is defined as,

$$\varepsilon^2 = \sum_{i=1}^{imax} \left(\mu_{di} - \mu_{mi}\right)^2 , \qquad \{11\}$$

where the index i ranges over the speeds of interest and *imax* is the total number of test points. The error-minimization requires the simultaneous solution of equations {3}, {4},

{6} and {7} for a wide range of the parameters α and β. The error-gradient information during this search suffers from numerical noise of this solution, and standard optimization procedures experience difficulty in finding the global minimum. Therefore, a *grid-search method* consisting of two sweeps is used. In the first sweep, a 10x10 grid of α and β values, covering a wide range of these parameters, are tested for each speed (i.e., each i in equation {11}). This gives the first-optimal (α, β) pair. Then, the ranges of α and β are refined around this solution by again choosing ten values for each one of the variables. The result of the second sweep is declared the optimal (α, β) pair that minimizes ε^2. These optimum values are tabulated in columns two and three of Table 4.

Testing the Effect of the Low Speed Kinetic Coefficient of Friction on the Optimal Values of Contact Parameters

Considering the uncertainty in the experimental value of μ_o, it was decided that an investigation of the effect of this parameter on the optimal values of α and β is warranted. Consider web 5 for which the experimentally measured μ_o value was 0.18 (Table 2). The effect of μ_o values of 0.15, 0.2, 0.25 and 0.3 on the optimum α and β was tested. The parabolic contact pressure parameters were tested in the ranges $1 \leq \alpha \leq 10$ μm and $5 \leq \beta \leq 45$ kPa. Figure 4 gives the contours of the squared-error ε^2, after the first-sweep, for these four μ_o values, for web-5. The optimal values of these tests are indicated on the plots. This figure shows that, as the error is reduced, the contours of ε^2 become essentially parallel to the β axis. This finding implies that the asperity compliance β has less influence on the error variation than the engagement height α. For the four different μ_o values, 0.15, 0.2, 0.25 and 0.3, the optimal values of β are 45, 15, 10 and 5 kPa, respectively, while the optimal α value remains at 4 μm. This result implies that the μ_o value too, has less influence on the error variation than α.

Similar tests were repeated for all of the webs and it was found that this characteristic is typical for all. The results of these tests for all eight web/roller combinations are summarized in columns 4-6 of Table 4. These columns represent the range of optimum values for α_m (column 4) and β_m (column 5) over the range of μ_o (column 6) tested. This table, like Figure 4, shows that the steady state equilibrium in the web-roller interface is influenced more significantly by the engagement height α, than by the compliance β or the coefficient of friction μ_o.

The conclusions reached above can be explained by investigating the influence of the asperity compliance β on the equivalent coefficient of friction μ_d, as a function of web speed V_W. Figure 5 gives μ_d-*vs*-V_W for β = 22.5 and 225 kPa. This figure shows that high asperity compliance (low β) results in a μ_d-*vs*-V_W variation that drops off more rapidly, than low compliance (high β). This behavior can be explained as follows; in the low-β case, the asperities deflect more, in order to apply the same contact pressure as the high-β case; more asperity deflection results in a lower web-roller clearance, which in turn causes higher air pressure build-up in the interface. Therefore, the webs with more compliant asperities lose more traction at a given web speed than the webs with stiffer asperities. However, as shown in Figure 5, a factor of ten difference in β causes a relatively small change in the μ_d-*vs*-V_W behavior. Hence, it is not surprising to find that β has a small influence on the μ_d variation, as was concluded in the previous paragraphs.

Engagement Height Based on Surface Topography

The error minimization analysis already gives α_c to be used as α in equation {3}, based on the results of the traction experiments. The goal in this section is introduce a measure of the engagement height, based on the easily measurable surface parameters, R_{pm} and R_z, that gives a good correlation with α_c. This is achieved in two parts: first, a model is proposed to calculate the engagement height of an individual surface based on the topography of the surface; second, a method is described for calculating the composite surface roughness of two surfaces coming in contact.

Proposed Model for Engagement Height Based on Surface Topography. Wu and Talke (1996) showed that a peak-to-valley surface roughness R_z worked well to predict the asperity engagement height α, when the contact of a rough tape and a smooth head is considered. While this appears to be true for magnetic tapes whose surface heights have a Gaussian distribution, the authors find that, in general, using R_z alone can be misleading. It is shown below that a combination of R_z and mean-peak-roughness R_{pm} describes α for the web-traction problem, especially for non-Gaussian surfaces, much better than R_z alone.

As explained above, if the contact clearance is narrow, when a web moves in contact with a roller, more air pressure will build-up in the interface. In fact, if the web can be made to rest on a few, relatively tall, localized asperities, then prevention of air pressure build-up will be more effective. In this respect, it can be said that the peaks on the surface are more effective than the valleys in preventing air pressure build-up. In order to illustrate this point **Figure 6** depicts three different surfaces: a surface with a few peaks in case-1, a surface with a few valleys in case-2 and a surface with equal number of peaks and valleys in case-3. These surface topographies are clearly non-Gaussian, yet they are encountered in many applications. When a smooth web comes in contact with the rollers in case-1 and case-2, the true engagement height is significantly larger for case-1, even though R_z is the same for both roller surfaces. Case-3 has an R_z twice as large as cases-1 and -2. The engagement height for case-3 is larger than that of case-1 but probably not twice as large, as R_z alone would suggest. This shows that for non-Gaussian surfaces R_z alone is not a good measure of the asperity engagement height α.

The R_z/R_{pm} ratio for the cases-1,-2 and-3 are approximately 1, much greater than 1 and approximately 2 respectively. In general, the R_z/R_{pm} ratio describes a rough surface as follows,

- $R_z/R_{pm} \cong 1$: only a few peaks and even fewer valleys,
- $R_z/R_{pm} >> 1$: only a few valleys and even fewer peaks,
- $R_z/R_{pm} \cong 2$: an equal number of peaks and valleys of nearly same amplitude.

It seems that a measure for α that combines R_z, R_{pm} and R_z/R_{pm} would be appropriate in order to capture these effects. To this end, the following heuristic model is proposed for estimating α when a smooth surface comes into contact with a rough surface,

$$\alpha = R_{pm} + \frac{\left(R_z - R_{pm}\right)}{\left(R_z / R_{pm}\right)} \qquad \{12\}$$

In this relation, α approaches: R_{pm} as $R_z/R_{pm} \cong 1$, $2R_{pm}$ as $R_z/R_{pm} >> 1$, and $0.5(R_z+R_{pm})$ as $R_z/R_{pm} \cong 2$. It is reasonable to assume that the surfaces with Gaussian distribution of asperities would have $R_z/R_{pm} \cong 2$, thus the engagement height $\alpha = 0.5(R_z+R_{pm})$, predicted by equation {12}, is only slightly lower than Wu and Talke's (1996) measurements. **Figure 7** illustrates the relation of α to R_z and R_{pm} and illustrates that $R_{pm} \leq \alpha \leq 2R_{pm}$.

Calculating the Composite Engagement Height of Two Surfaces in Contact. For the eight/web/roller combinations studied in this paper, the roughness of both surfaces are significant. Therefore, it is reasonable to expect that a composite engagement height α_c, used in equation {3}, would need to include the effects of the roughness of both surfaces. For Gaussian surfaces, α_c can be obtained by the root-mean-square (rms) of the engagement heights of the two surfaces (Bhushan, 1996). This may not be applicable in general. Therefore, the following three functions were tested for calculating the composite engagement height,

$$\alpha_c = \begin{cases} \alpha_r + \alpha_w & :\texttt{sum-model} \\ \sqrt{\alpha_r{}^2 + \alpha_w{}^2} & :\texttt{rms-model} \\ max(\alpha_r, \alpha_w) & :\texttt{max-model} \end{cases} \qquad \{13\}$$

where the roller engagement height α_r and the web engagement height α_w are calculated using equation {12}. In order to see why these forms are appropriate, consider the idealized surfaces presented in Figure 9. Case-1 presents surfaces for the *sum-model*: in this case, the roller has a surface comprised of high frequency roughness with equal peaks and valleys, while the web has a few peaks. Case-2 presents surfaces for *rms-model*: in this case, both the web and the roller have high frequency roughness with equal peaks and valleys. Case-3 is the *max-model* where both the web and roller have a few peaks and valleys.

Table 5 shows the composite engagement height values α_c calculated using equations {12}, and {13} with the measured values from Table 3, and the sum and rms of R_z. The engagement height values α_m determined after error-minimization as described above are repeated from Table 4. Comparison of the three α_c and the two R_z values given in this table with the optimized engagement heights α_m shows that for webs-1, -5 and -8 the rms-model, and for the other webs the sum-model is applicable. None of the webs require the use of the max-model. The choice of the appropriate model for each web is underlined.

The appropriate choices indicated in the above paragraph are not arbitrary, but depend on the nature of the web and roller roughness. The nature of these contact heights can be unraveled by studying Figure 8 which shows the surface topography of webs-1,-7, and -8

and the roller, obtained with the optical surface profiler. Note that the surface of web-7 is representative of webs-2,-3,-4, and –6. This figure shows that the roughness of web-1 and web-8 are more evenly distributed, indicating a Gaussian distribution. In fact the R_z/R_{pm} ratio for webs-1 and –8 from Table 3 is 1.8. On the other hand, web-7 shows more individual peaks and has $R_z/R_{pm} = 1.2$. Finally, the roller shows more valleys than peaks and its R_z/R_{pm} ratio is 5.33. Thus it can be seen that the interface of web-1 (web-8) and the roller is similar to the case-2 depicted in Figure 9, and the interface of web-7 and the roller is similar to case-1 of the same figure.

The results presented in Table 5 indicate that in calculating the composite engagement height of a roller that has a high R_z/R_{pm} ratio and a web, the sum-model is appropriate if the web surface has $1.1 \leq R_z/R_{pm} < 1.4$ and the rms-model is appropriate if the web surface has $1.4 \leq R_z/R_{pm} \leq 1.8$. While the limits for this methodology are somewhat arbitrary, observation of Table 5 shows that the procedure works well for all of the webs in this study. The results also show that peak-to-valley roughness measures do not work as well. The final two columns in Table 5 show the sum and rms combination of the web and roller R_z and in all cases, the results are too high.

THE EFFECT OF ENGAGEMENT HEIGHT ON TRACTION

The ability of the proposed model presented in this paper to accurately predict roller traction is shown in Figure 10. For each of the eight webs of this study, the experimental speed at 50% traction loss is shown plotted against the predicted speed using the rms and sum asperity composite models. As can be seen, the predictions from the model accurately predict the experimental results. The data also shows clearly for each web which roughness model is most appropriate.

Figure 11 shows the predicted equivalent coefficient of friction vs. speed using each of the three estimates for the asperity engagement height. Results are shown for all eight webs. For webs 2, 3, 4, 6 and 7 the estimated β_m values are used, while for the remaining webs the β_m values obtained from compressibility measurements are used. Also shown are the experimental data measured on the dynamic traction tester. It is again seen that in all cases the most appropriate asperity engagement model gives the best agreement to the optimum predictions. Further, in most cases, the agreement to the experimental data is very good. The only exception is the last case, web 8. In this case, the model is shown to overpredict the equivalent coefficient of friction.

SUMMARY

An analytical model has been presented which predicts smooth roller traction as a function of speed. The model uses a simple two parameter contact model which expresses the relationship between the web-roller clearance and contact pressure. The traction loss over a roller was characterized experimentally for eight webs of different roughness characteristics. An error-minimization procedure was used to estimate the asperity engagement height and compliance for the parabolic contact model from the traction experiments. A heuristic model was developed to compute the asperity engagement height based on R_{pm} and R_z when one or both surfaces are rough. It was shown that the appropriate model depends on the web and roller surface characteristics.

A method was presented for selecting the appropriate model. A method was also presented to estimate the asperity compliance, which for the web and roller combinations studied in this paper, has only a secondary effect on the equivalent coefficient of friction. The results of this work confirmed that webs with high, distributed asperities perform better against traction loss.

REFERENCES

1. ASTM Standard G143-96, "Standard Test Method for Measurement of Web/Roller Friction Characteristics," Annual Book of ASTM Standards, 1996.
2. Bhushan, B., Tribology and Mechanics of Magnetic Storage Devices, Springer-Verlag Inc., New York, 1996.
3. Burgdorfer, A., "The Influence of the Molecular Mean Free Path on the Performance of Hydrodynamic Gas Lubricated Bearings," Journal of Basic Engineering, Trans. of the ASME, March 1959, pp. 94-100.
4. Daly, D.A., "Factors Controlling Traction Between Webs and Their Carrrying Rolls," Tappi Journal, Vol. 48, No. 9, Sept. 1965, pp. 88-90.
5. Ducotey, K.S., Good, J.K., "The Importance of Traction in Web Handling," Trans. ASME, Journal of Tribology, Vol. 117, Oct. 1995, pp. 679-684.
6. Eshel, A., Elrod, H.G. Jr., "The Theory of the Infinitely Wide, Perfectly Flexible, Self-Acting Foil Bearing," ASME Journal of Basic Engineering, Dec. 1965, pp. 831-836.
7. Forrest, A.W. Jr., Anderson, V.L., "Film Surface Considerations for Enhancing Winding of Thin Films," Proceedings of the Fourth International Conference on Web Handling, Oklahoma State University, June 1997.
8. Greenwood, J.A., Tripp, J.H., "The Contact of Two Nominally Flat Rough Surfaces," Proc. Instn. Mech. Engrs., Vol. 185, 1970-1971, pp. 625-633.
9. Gross, W.A., Fluid Film Lubrication, John Wiley & Sons, N.Y., 1980.
10. Knox, K.L., Sweeney, T.L., "Fluid Effects Associated with Web Handling", Ind. Eng. Chem. Process Des. Develop., Vol. 10, No. 2, 1971, pp. 201-205.
11. Müftü, S., Altan, M.C., "Mechanics of a Porous Web Moving Over a Cylindrical Guide," in review Journal of Tribology, Trans. ASME, May 1999.
12. Müftü, S., Benson, R.C., "Modelling the Transport of Paper Webs Including the Paper Permeability Effects", Advances in Information Storage and Processing Systems, ASME International Mech. Eng. Congress and Exposition, San Francisco, CA., ISPS-Vol. 1, 1995, pp. 247-258.
13. Müftü, S., Benson, R.C., "A Study of the Cross-Width Variations in the Two Dimensional Foil Bearing Problem," Trans. ASME J. of Tribology, Vol. 118, 1996, pp. 407-414.
14. Müftü, S., Cole, K.A., "The Fluid/Structure Interaction in Supporting a Thin Flexible Cylindrical Web with an Air Cushion," in review Journal of Fluids and Structures, Sept. 28, 1998.
15. Wu, Y., Talke, F., "The Effect of Surface Roughness on the Head-tape Interface", Trans. ASME, Journal of Tribology, Vol. 118, No. 2, April 1996, pp. 376-381.

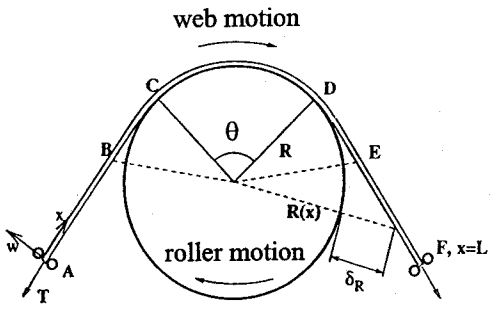

Fig. 1 Schematic view of a web conveyed over a cylindrical rotating roller.

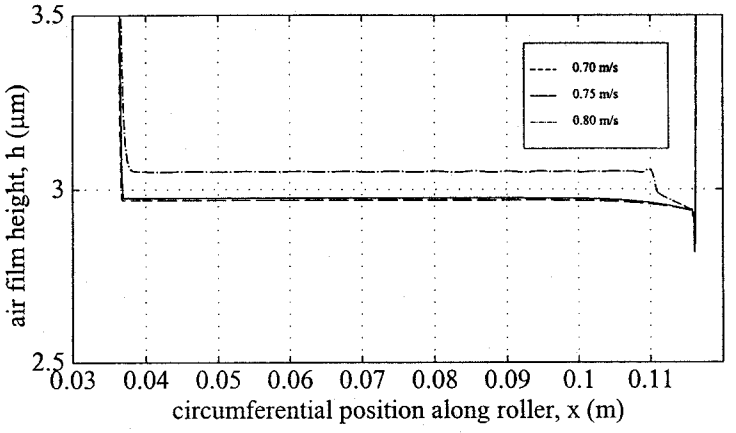

Fig. 2 Finite difference code vs. foil bearing: Foil bearing equation predicts an air film height of 3 μm at 0.74 m/s.

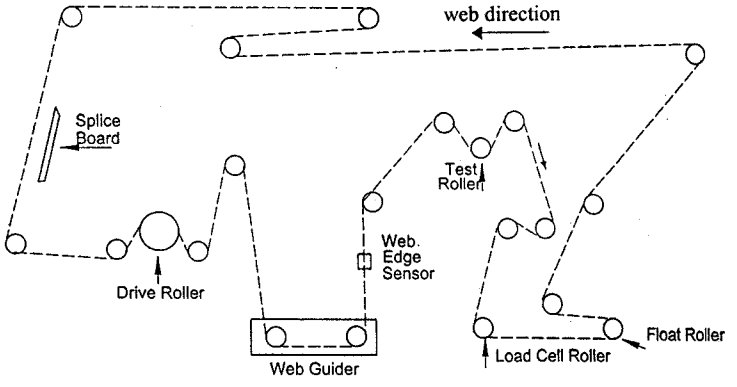

Fig. 3 Schematic of the dynamic traction tester.

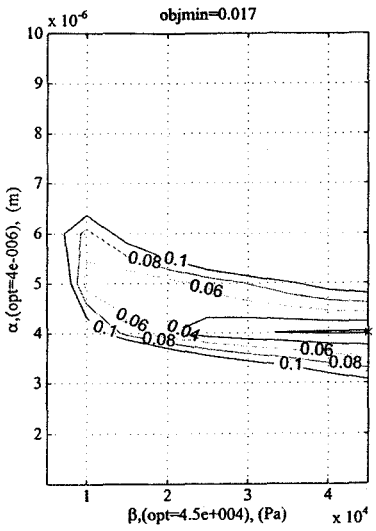

(a) case 1: $\mu_0 = 0.15$

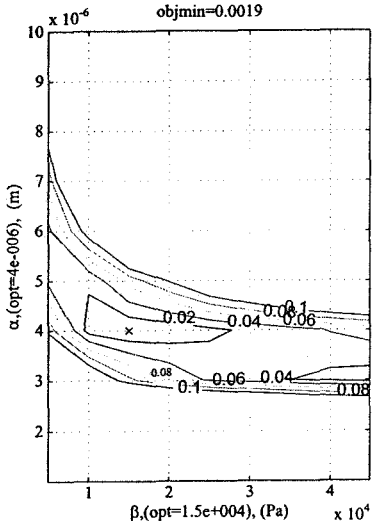

(b) case 2: $\mu_0 = 0.20$

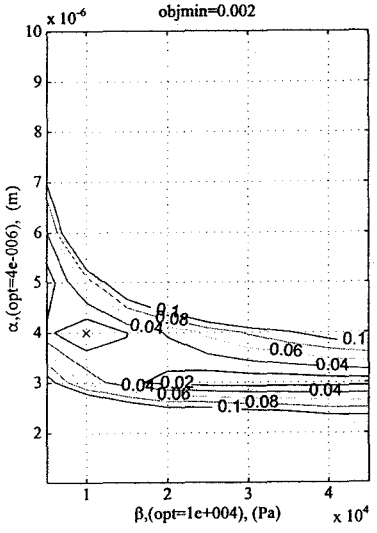

(c) case 3: $\mu_0 = 0.25$

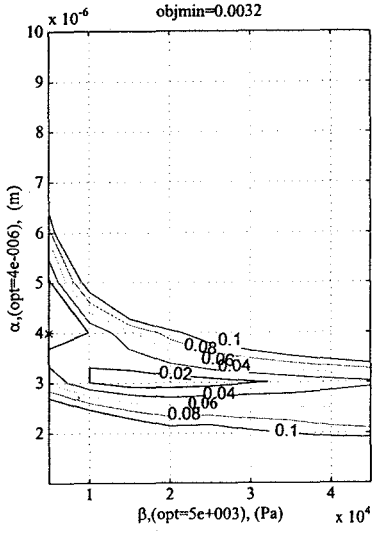

(d) case 4: $\mu_0 = 0.30$

Fig. 4 Optimization contours for web number 5 for various μ_0. Optimum locations are indicated by "x" symbols.

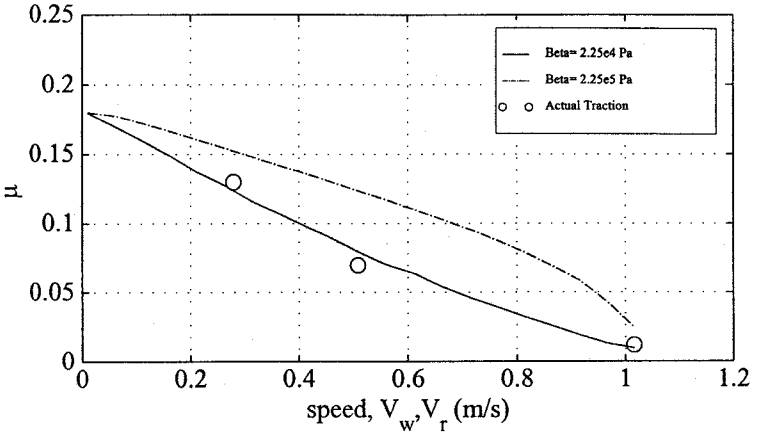

Fig. 5 Predicted traction curves for high β vs. low β.

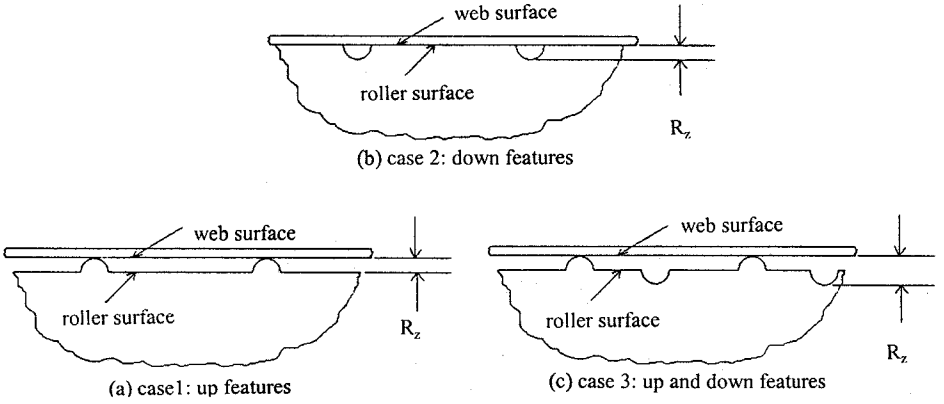

Fig. 6 Pictorial view of contact between a smooth web and various idealized roller surface textures.

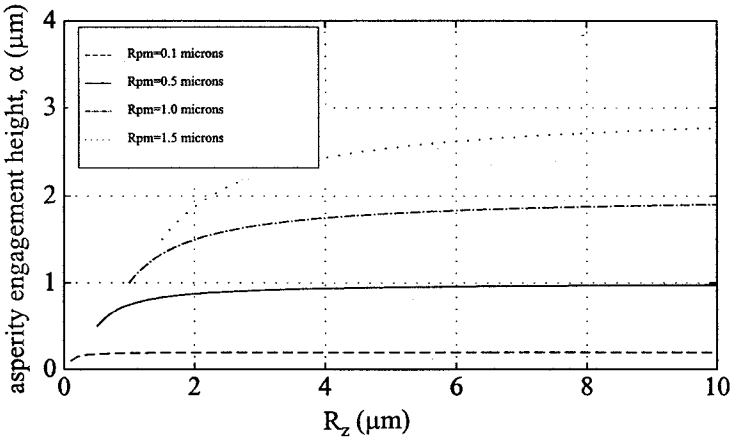

Fig. 7 Surface roughness model prediction of how α varies with R_z for different R_{pm} values (equation 12).

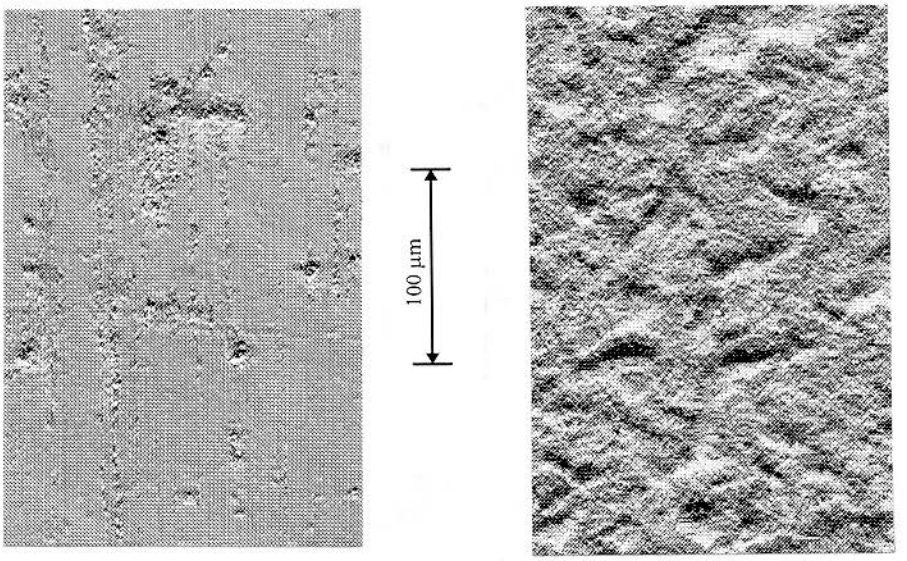

(a) roller, R_z/R_{pm}=5.33

(b) web number 1, R_z/R_{pm}=1.8

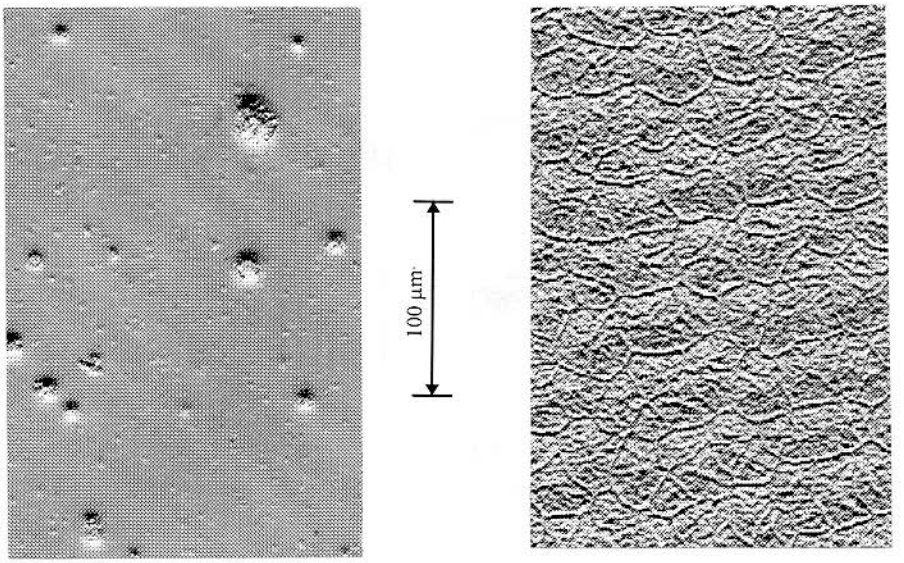

(c) web number 7, R_z/R_{pm}=1.2

(d) web number 8, R_z/R_{pm}=1.8

Fig. 8 Visualization of surface topography using non-contact interferometry at a magnification of 250x.

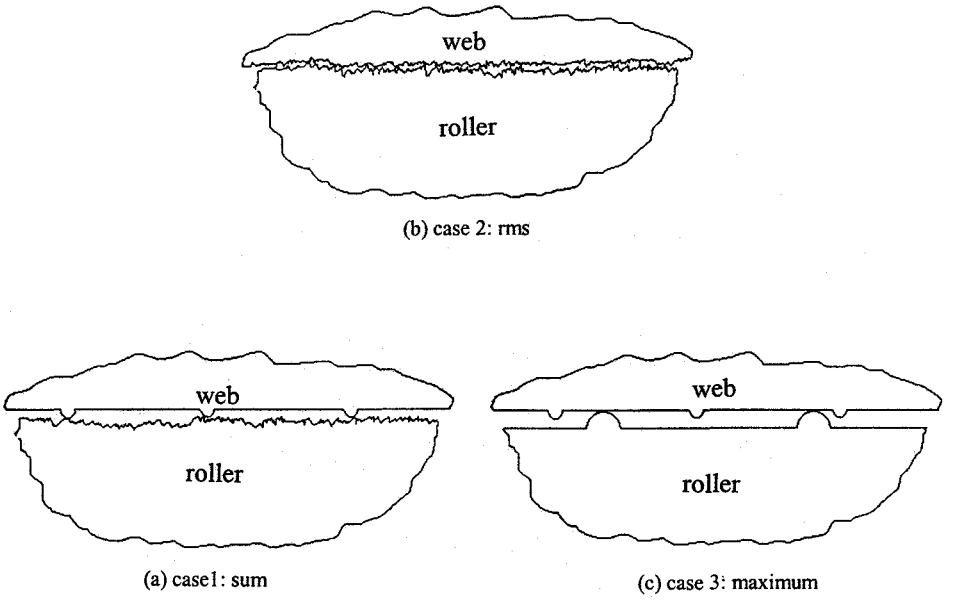

Fig. 9 Pictorial view of how two rough surfaces might combine for various surface textures (see equation 13).

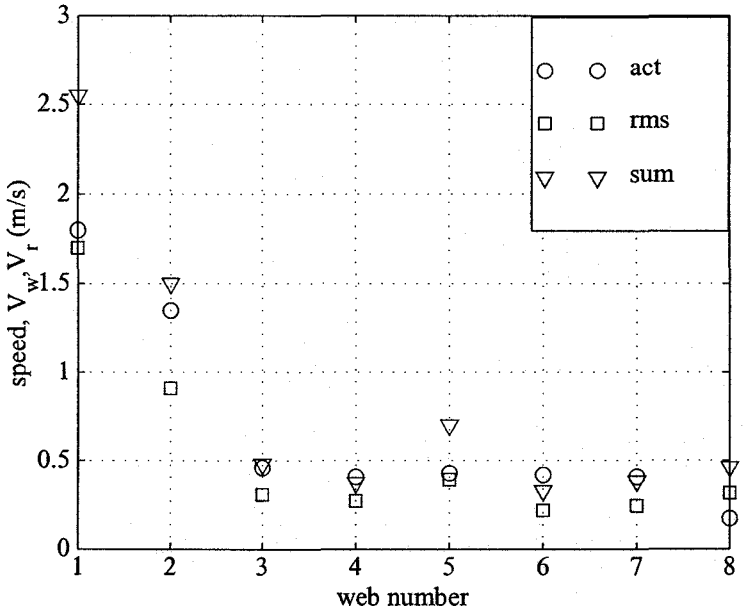

Fig. 10 Speed (V_w,V_r) at which the value of coefficient of friction, μ, is reduced by 50% of it's initial value, μ_o.

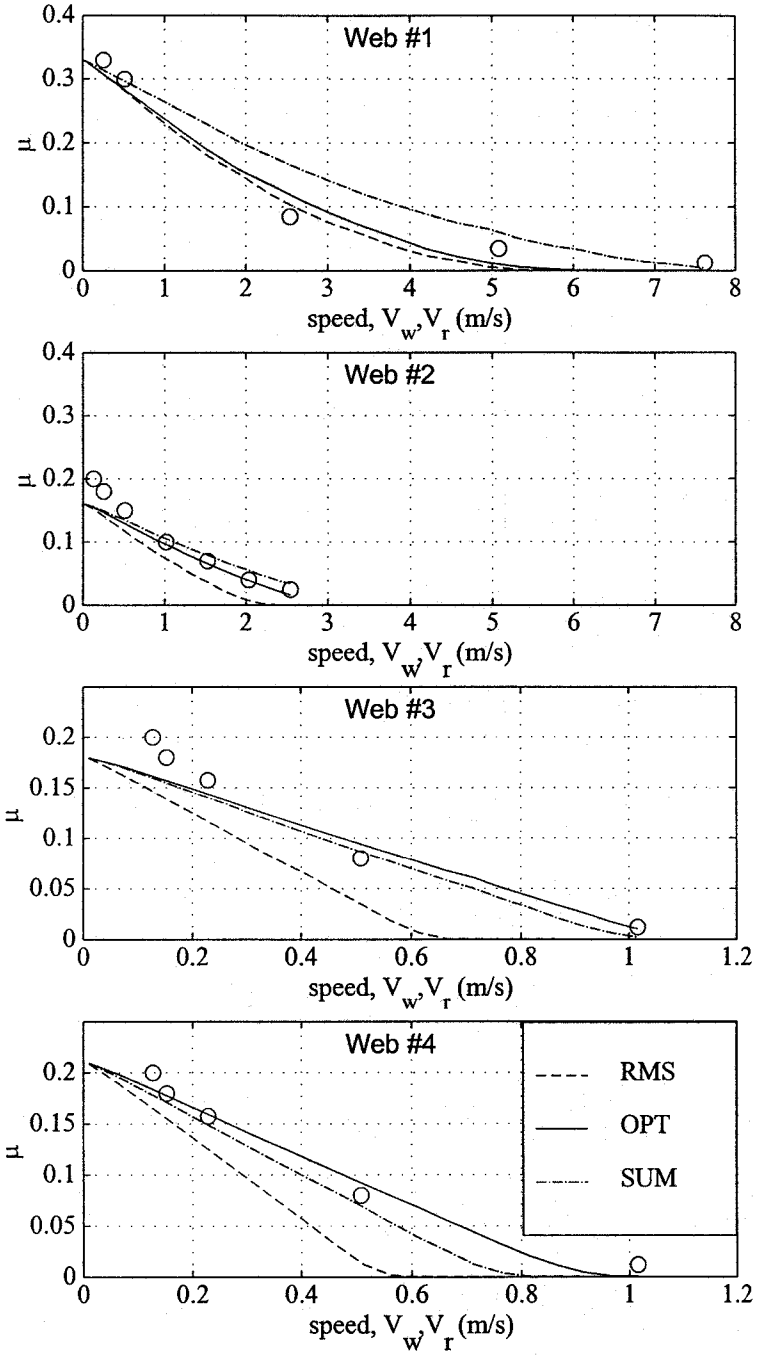

Fig. 11 Equivalent coefficient of friction: model prediction, μ_m, vs. actual measured, μ_d.

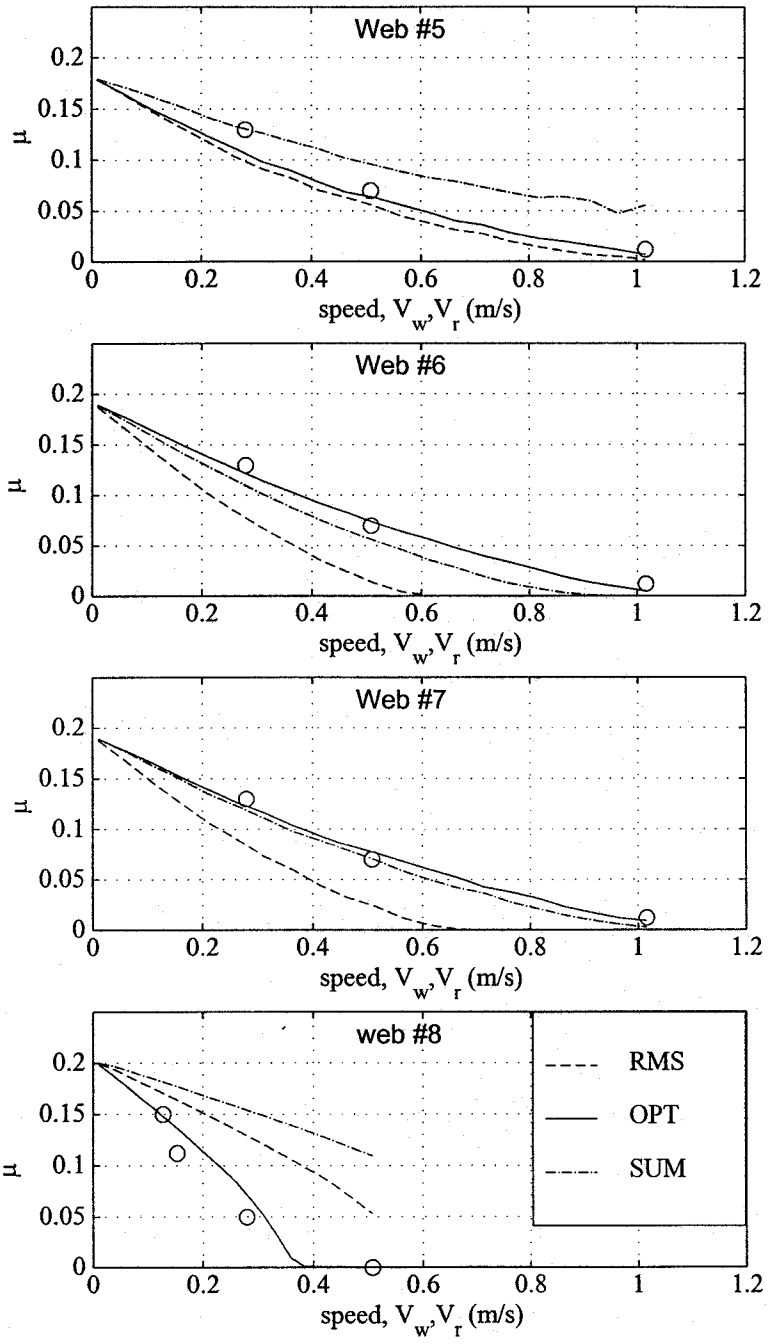

Fig. 11 Continued from previous page.

Table 1-Web description

web #	description	thickness (μm)	width (m)	density (kg/m^3)	Young's Modulus (Pa)
1	Polyethylene coated paper	272	0.75	1108	4.14E+09
2	coated Polyethylene Terephthalate	182	0.75	1358	4.83E+09
3	coated Polyethylene Terephthalate	179	0.75	1358	4.83E+09
4	uncoated Polyethylene Terephthalate	98	0.75	1358	4.83E+09
5	coated Polyethylene Terephthalate	183	0.75	1358	4.83E+09
6	coated Cellulose Triacetate	122	0.75	1358	4.14E+09
7	coated Polyethylene Terephthalate	176	0.75	1358	4.83E+09
8	coated Polyethylene Terephthalate	118	0.75	1358	4.83E+09

Table 2-Coefficient of friction experimental data

Dynamic traction test conditions:

0.102 m dia. roller with 90 degree wrap

0.75 m wide web at 175N/m unit tension

	traction coefficient (web ID,speed)							
speed (m/s)	web 1	web 2	web 3	web 4	web 5	web 6	web 7	web 8
0.005[a]	*0.21*	*0.16*	*0.18*	*0.21*	*0.18*	*0.19*	*0.19*	*0.20*
0.13		0.20	0.20	0.20				0.15
0.15			0.18	0.18				0.11
0.23			0.16	0.16				
0.25	0.33	0.18						
0.28					0.13	0.13	0.13	0.05
0.51	0.30	0.15	0.08	0.08	0.07	0.07	0.07	0.00
1.02		0.10	0.01	0.01	0.01	0.01	0.01	
1.52		0.07						
2.03		0.04						
2.54	0.09	0.03						
5.08	0.04							
7.62	0.01							

a. All 0.005m/s speed traction coefficients are from ASTM G143 test. The 95% confidence limits on the mean for the ASTM G143 tester are +/- 0.01. All other traction coefficients are from the dynamic traction test.The 95% confidence limits on the mean for the dynamic traction test are +/- 0.01.

Table 3-Surface roughness data

	R_{pm}			R_z		
	mean	std	+/-95% c.l.	mean	std	+/-95% c.l.
	(μm)	(μm)	(μm)	(μm)	(μm)	(μm)
web 1	6.08	0.62	0.99	10.88	0.60	0.96
web 2	4.99	0.62	0.98	5.74	0.66	1.05
web 3	1.04	0.14	0.22	1.22	0.20	0.32
web 4	0.61	0.30	0.48	0.72	0.32	0.51
web 5	2.07	0.18	0.28	2.98	0.10	0.16
web 6	0.80	0.08	0.13	0.99	0.14	0.22
web 7	1.03	0.18	0.29	1.24	0.23	0.36
web 8	0.68	0.06	0.10	1.20	0.10	0.16
roller	1.44	0.12	n/a	7.67	2.09	n/a

Number of samples equals 4 for webs and 2 for roller.

Table 4- Optimized engagement height and compliance

	α_m	β_m	α_m range	β_m range	μ_o range
	(μm)	(Pa)	(μm)	(Pa)	
web 1	9.5	20000	8.0 - 10.0	5000 - 40000	0.30 - 0.45
web 2	7.5	27500	7.0 - 9.0	5000 - 45000	0.15 - 0.30
web 3	4.0	40000	4.0 - 4.5	5000 - 45000	0.15 - 0.30
web 4	3.7	37500	4.0 - 4.5	5000 - 45000	0.15 - 0.30
web 5	4.0	22500	4.0 - 4.0	5000 - 45000	0.15 - 0.30
web 6	4.0	17500	4.0 - 4.0	5000 - 45000	0.15 - 0.30
web 7	4.0	17500	4.0 - 4.0	5000 - 45000	0.15 - 0.30
web 8	2.0	40000	2.0 - 2.5	10000 - 40000	0.15 - 0.30

Table 5- Model engagement height vs. optimum

	α_m	α_c sum	α_c rms	α_c +/-95% c.l.	α_w mean	α_w std	R_z/R_{pm} web	R_z sum	R_z rms
	(μm)	(μm)	(μm)	(μm)	(μm)	(μm)		(μm)	(μm)
web 1	9.5	11.4	9.1	1.4	8.8	0.6	1.8	18.6	13.3
web 2	7.5	8.3	6.2	1.4	5.6	0.5	1.1	13.4	9.6
web 3	4.0	3.8	2.9	0.6	1.2	0.2	1.2	8.9	7.8
web 4	3.7	3.3	2.7	0.8	0.7	0.2	1.2	8.4	7.7
web 5	4.0	5.3	3.8	0.4	2.7	0.1	1.4	10.6	8.2
web 6	4.0	3.6	2.8	0.6	1.0	0.1	1.2	8.7	7.7
web 7	4.0	3.8	2.9	0.7	1.2	0.2	1.2	8.9	7.8
web 8	2.0	3.6	2.8	0.5	1.0	0.1	1.8	8.9	7.8
roller					2.61[a]	0.21[a]	5.33		

a. These are α_r not α_w values.

B. S. Rice, K. A. Cole And S. Müftü
An Experimental And Theoretical Study of Web Traction Over a Nonvented Roller
6/9/99 Session 4 1:50 - 2:15 p.m.

Question:
Do you apply a braking force to your test roller?

Answer – B. S. Rice, Kodak
Yes. We apply a torque to the test roller.

Comment – Keith Good, Oklahoma State University
We note that the static coefficient of friction is actually less than the kinetic coefficient of friction.

Answer – B. S. Rice, Kodak
We have seen the same thing, but the difference between the static coefficient and kinetic is usually very small. Either the static or kinetic coefficient of friction can be used in the model.